Proceedings of the XVII ECSMGE-2019
Geotechnical Engineering foundation of the future
ISBN 978-9935-9436-1-3

doi: 10.32075/17ECSMGE-2019-0978

XVII European Conference
ECSMGE 2019
Reykjavik
on Soil Mechanics
and Geotechnical Engineering

Multiscale analysis of active state failure behind a retaining wall

Analyse à plusieurs échelles de la défaillance d'un état actif derrière un mur de soutènement

B. Soltanbeigi
Institute for Infrastructure and Environment, University of Edinburgh, EH9 3JL, Edinburgh, UK

A. Altunbas
Department of Architecture, Istanbul Medipol University,34815, Istanbul, Turkey

O. Cinicioglu
Department of Civil Engineering, Bogazici University, 34342, Istanbul, Turkey

ABSTRACT: Discrete element method (DEM) simulates the interaction of particulate material by tracking the displacement and calculation of force for individual grains. Current study, initially simulates the active state failure behind a retaining wall for a cohesionless backfill. The considered particles are differentiated by shape parameter; both spherical and non-spherical particles are included.
Additionally, a physical lab-scale model retaining wall that can reproduce active state failure is utilized in this study. Tests are performed on a uniformly graded local sand (Akpinar sand). The model has transparent wall which will allow the observation of the deformation during the test. Eventually, failure surface evolution from DEM simulations is compared qualitatively to those of experimental observations. Obtained results suggest that it is crucial to incorporate non-spherical particles for DEM simulations to enable realistic representation of a granular backfill.

RÉSUMÉ: La méthode des éléments discrets (DEM) simule l'interaction des particules en suivant le déplacement et le calcul de la force pour chaque grain. L'étude actuelle simule d'abord la défaillance de l'état actif derrière un mur de soutènement pour un remblai sans cohésion. Les particules considérées sont différenciées par le paramètre de forme; les particules sphériques et non sphériques sont incluses.
De plus, un modèle de mur de soutènement physique à l'échelle du laboratoire capable de reproduire une défaillance d'état actif est utilisé dans cette étude. Les tests sont effectués sur un sable local uniformément classé (sable Akpinar). Le modèle a une paroi transparente qui permettra d'observer la déformation au cours de l'essai. Finalement, l'évolution de la surface de défaillance à partir des simulations DEM est comparée qualitativement à celle d'observations expérimentales. Les résultats obtenus suggèrent qu'il est crucial d'incorporer des particules non sphériques dans les simulations DEM afin de permettre une représentation réaliste d'un remblai granulaire.

Keywords: DEM; Particle shape; Retaining wall; Physical model; Active state

1 INTRODUCTION

Retaining walls, as one of the most demanding infrastructures, are designed for various applications, such as: flood or avalanche prevention barriers, slope stability in highways and bridge abutments. The main factor contributing in efficient and safe design of soil retaining structures is the magnitude of the induced forces from the embankment. The conventional designing procedures proposed by Coulomb (1776) and Rankine (1857) assume linear distribution of the earth pressures that leads to consideration of resultant pressure at the one third of the wall height from the toe, which is in contrary to the results presented in recent studies. Moreover, experimental evidence clearly shows that the failure planes associated with resulting failure wedges are not linear. In spite of numerous experimental and numerical studies that have been conducted to understand the distribution of lateral earth pressures and the geometry of associated failure wedges, there are still discrepancies between the solutions and real behaviour of the granular assemblies.

Many researchers made assumptions regarding the geometry of the slip plane with the intention of investigating the lateral earth pressure and its distribution (Terzaghi 1943, Toyosawa et al. 2006, Goel and Patra 2008). Results obtained in these studies are dependent on the validity of the assumed failure surface geometries. Terzaghi (1943), investigating the results of model tests, suggested a curvilinear failure surface. Later, Tsagareli (1965) experimentally investigated fixed walls and proposed curvilinear failure surfaces that can be mathematically defined with a power function. Spangler and Handy (1982), agreeing with Tsagareli on the curvilinear nature of failure surfaces, proposed a parabolic function for their quantification. Toyosawa et al. (2006) conducted centrifuge model tests using a movable earth support apparatus, investigating the influence of mode of wall movement on the geometry of failure surfaces. The results of their study suggested that different modes of wall movement lead to different failure surface geometries. Pietrzak and Lesniewska (2012) performed model tests to evaluate and observe active failure in granular materials retained by rigid walls using Particle Image Velocimetry method (PIV). Based on the PIV results, they suggest that curvilinear failure surfaces are generated behind retaining walls.

Even though there is no consensus over the general shape of the active failure plane, it is an established fact that its geometry is affected by many factors, such as the properties of the backfill, the imposed stress state, and the mode of wall movement. In model tests changing boundary conditions is straightforward, however, varying particle-scale soil properties is limited. Meanwhile, utilization of numerical methods enhances conduction of such systematic studies.

Among popular numerical techniques, the Discrete Element Method (DEM), developed by Cundall and Strack (1979), has been successfully used for predicting the behaviour of granular materials. DEM considers the granular material as a system of distinct interacting bodies and provides an insight into its overall response. Our study considers the so-called soft contact approach, in which particles are assumed rigid for shape definition purpose, and also allowed to overlap during contact (an elastic deformation). A detailed description of the work process on DEM can be found in the literature (O'Sullivan 2011).

Among the diverse physical properties of individual particles in particulate materials, the shape and surface morphology play an important role in the development of shear strength and failure. Obviously, this dependency is due to the direct influence of these factors on the inter-particle interactions at micro-scale. To analyse the effect of shape on the granular flows, several approaches have been utilized in DEM, such as clumped spheres, superquadrics (Soltanbeigi et al. 2018) and polyhedral shapes.

Clumped spheres, which approximate the shape of particles by overlapping or touching of spheres, are used as approximation of the real

shape irregularities (Favier et al. 1999) The centres of individual spheres are located at a constant relative distance and the size of adjacent particles may vary to produce complex shapes.

Spheres are the most preferred type of geometry for representing particles due to the simplicity in the method of contact detection and force calculation. The distance between two adjacent spheres determines the contact; if the centre-to-centre interval of adjacent particles becomes less than the sum of both radii, then particles are considered as in contact. Besides, the efficiency and accuracy in the evaluation of contact overlap is another superiority of the spheres that provides a distinct computational performance. Consequently, these outstanding features provide quick and precise assessment of contact forces in the system. Regarding these properties of spheres, it is always of interest to replicate complex shaped granular assemblies using this simple geometry (Wensrich and Katterfeld 2012).

In the current study the dependency of slip surface geometry on soil density is investigated by conducting tests on 1 g small-scale retaining wall model. Having transparent sidewalls, PIV is employed to visualize the evolution of slip surface and determine its geometric characteristics.

Moreover, using DEM, a preliminary study is conducted to evaluate the capability of simple shape representation methods in capturing the macro-scale characteristics during active state. In this regard, a series of DEM simulations are performed within a model retaining wall with two types of particles; perfect sphere and non-spherical particle, which is composed of two overlapping spheres. Consequently, the results of DEM simulations and experimentally observed slip surfaces are qualitatively compared.

2 METHODOLOGY

2.1 Numerical model

A cohesionless retained backfill that deforms under a plane strain boundary condition is modelled using DEM, as shown in Figure 1a (Soltanbeigi et al. 2016). The retaining wall has a rough surface and its outward horizontal translation leads to active state failure. The proposed geometry has a periodic boundary in the depth of the backfill (*y* direction). Furthermore, the adverse influence of bed boundary effects is minimized by considering a layer of particles in the bottom section of the model. The properties of the particles in this layer are the same as in the backfill and its height is 10 times the mean particle diameter. Table 1 summarizes the list of parameters of the DEM simulation. The EDEM particle simulation software is used for running numerical simulations (DEM Solutions Ltd. 2014).

The initial step in DEM is to define the geometry of the system, where particles are free to overlap while they come into contact. Repeated calculations in DEM are performed with using Newton's second law, applied to the particles, and force-displacement law at the contacts. Force-displacement law relates the acting forces at the contacts among particles to the resulting displacements, in other words, it is used to calculate forces from displacements. The total normal and shear forces acting on every individual particle are calculated at each time step the by taking into account both the contact forces and body forces acting on the particle. Newton's second law of motion is applied after determination of the contact forces to each particle. Between two succeeding time-steps, it provides the acceleration, velocity and displacements of each element. For particle *i* the equation of motion is given by Equation (1):

$$m_i \frac{d^2}{dt^2} x_i = f_i + m_i g \tag{1}$$

where m_i is the mass of the particle, *t* is time, x_i is its position, g is the acceleration due to gravity and f_i is the force acting on the particle due to particle contacts and defined as Equation (2):

$$f_i = \sum_c f_i^c \tag{2}$$

The rotational motion equation for particle *i* is given by:

$$I_i \frac{d}{dt}\omega_i = T_i \quad (3)$$

where I_i is the moment of inertia for particle i, ω_i is its angular velocity and T_i is the total torque acting on it, which is defined by Equation (4) where l_i is the branch vector of particle i, defined by Equation (5):

$$T_i = \sum_{i=1}^{N_c} l_i^c \times f_i^c \quad (4)$$

$$l_i = r_i - r_j \quad (5)$$

The theory of DEM and its work process for calculating the position and force for individual particles is available in the literature [10] and will not be repeated here.

When using spherical particles, the granular system consists of 22000 spherical particles with a mean diameter of 3 mm and a standard deviation of 0.3 mm. We have also used the simplest multi-sphere particle, which is composed of two overlapping spheres and will be referred to as paired particle for rest of the paper. The total number of paired particles is approximately 18000 and the aspect ratio is 1.25, see Figure 1b.

The wall is translating with a constant speed of 1 mm/s to ensure the quasi-static flow of the particulate system. The particle data is saved with a frequency of 200 Hz.

2.2 Hybrid PIV-DEM strain measurement

Particle Image Velocimetry (PIV) is a numerical method for the determination of deformations through consecutive images taken from a transparent side of a sample. This technique was developed initially by Adrian (1991) for the field of experimental fluid mechanics.

This study uses GeoPIV for image analysis, which is a MATLAB module developed especially for applying PIV in geotechnical applications (Take et al. 2003). GeoPIV tracks the texture of the soil within captured images and provides displacement vector fields, shear and volumetric strain maps throughout the test.

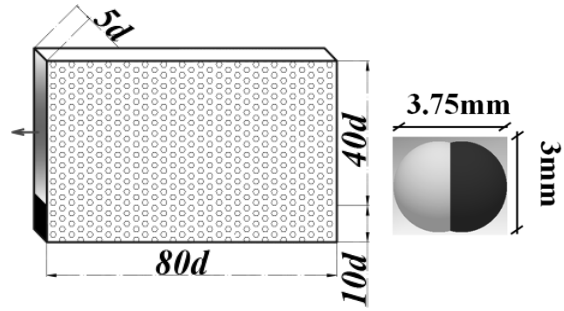

(a) (b)

Figure 1. DEM model a) geometry of the retaining wall and modelled backfill b) paired particles.

The first step in GeoPIV is to determine the area of interest (AOI) and cut it out of the digital image and divide into a grid of square patches, see Figure 2a. These patches are distinguished by their unique pixel intensity variation signatures. Subsequently, GeoPIV algorithm searches in a specified zone within the deformed image to find a patch that has maximum similarity to the initial patch's signature. The difference between the target patch, measured in pixels, and the reference patch is visualized by the displacement vector as shown in Figure 2b. The size of patches is also an important factor in the calculation of strain, as a result an optimum grid size is essential. According to Lesniewska and Wood (2009), the best solution to address related concerns is to consider relatively big, but overlapping patches. Here, we consider patches with size of 150 pixels and centre-to-centre distance of neighbouring patches of 50 pixels.

2.3 Small scale retaining wall model

The testing box is 140 cm in length, 60 cm in depth, and 50 cm in width and simulates plane strain condition, see Figure 3. Sides of the testing box are made of 20 mm thick Plexiglass, which are loaded by lateral pressures, allowing the observation and monitoring of the soil deformations.

As a result, photographic images of the backfill at different stages of wall deformation can be captured for using in later analysis. Captured images are analysed using PIV method for identifying the geometry of failure surfaces. The model wall is capable of translating laterally either towards or away from the retained backfill. The properties for the sand are summarized in Table 2.

2.4 Determination of failure surfaces

Using shear strain maps, slip surface can be identified by following the locus of maximum strain points. Accordingly, a coordinate system with its origin located at the bottom of the model wall is established in order to be able to quantify slip plane geometry, see Figure 4. Furthermore, established coordinate system is normalized by model wall height (H_w). Then, unit-independent quantification of the failure surface becomes possible. X and Y coordinates of the points along the slip plane are measured as shown in Figure 4. In this respect, outer edge of failure surfaces is marked with coloured dots and quantified for both *B* (away from the model wall) and *H* (along the length of the model wall) directions as shown in Figure 4.

3 RESULTS

This section covers the results obtained both from DEM simulations and conducted experiments.

The initial comparison provides a clear picture regarding the formed wedges during active failure, see Figure 5. The particles in DEM simulations are coloured according to horizontal velocity, whereas deformations are presented with a vector field for the experiments. It is seen that spherical particles fail to represent a proper failure wedge, while paired particles provide a similar failure to that of experiments.

Table 2. Mechanical properties of Akpinar Sand.

Property	Value
D_{50}	0.27
Uniformity coefficient, (C_u)	1.23
Coefficient of gradation, (C_c)	0.97
Average sphericity, (S_{ave})	0.7
Average roundness, (R_{ave})	0.5
Critical state friction angle	33

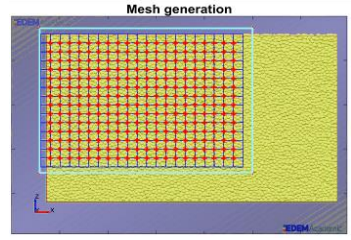

(a)

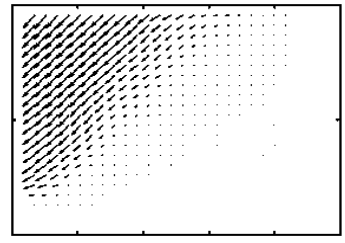

(b)

Figure 2. Graphical representation of PIV a) AOI and patches b) vector field for the deforming media.

Table 1. Model parameters used in the DEM simulations

Parameter	Symbol	Unit	Value
Mass density	ρ	kg/m^3	950
Shear modulus	G	Pa	1E+08
Friction coefficient (particle- geometry)	$\mu_{P\text{-}G}$	-	0.5
Friction coefficient (particle- particle)	$\mu_{P\text{-}P}$	-	0.577
Mean radius of the spheres	r	mm	1.5

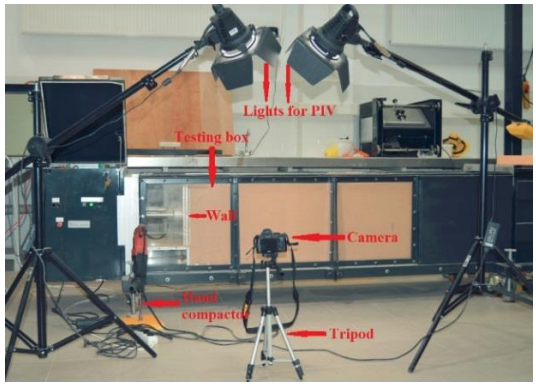

Figure 3. Test set-up.

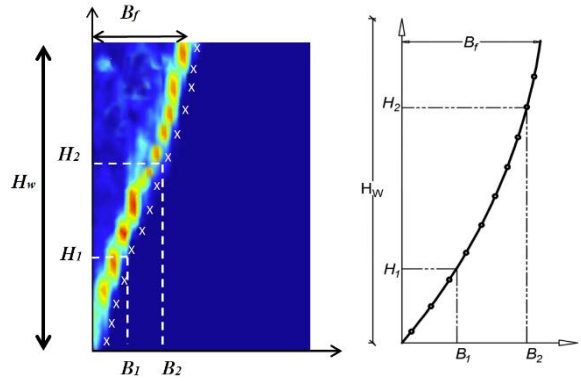

Figure 4. Quantification of Slip Plane Geometry.

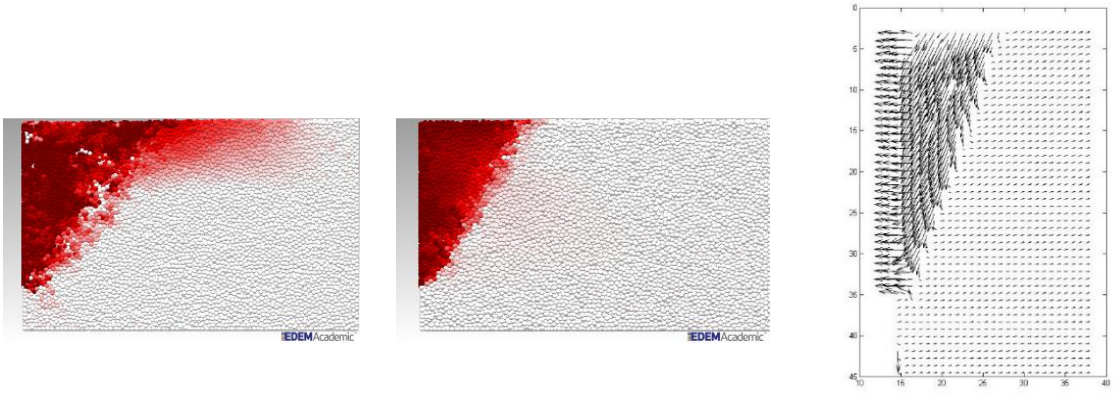

(a) (b) (c)

Figure 5. Displacement of backfills with a) spheres (DEM) b) paired particles(DEM) c) PIV (experimental).

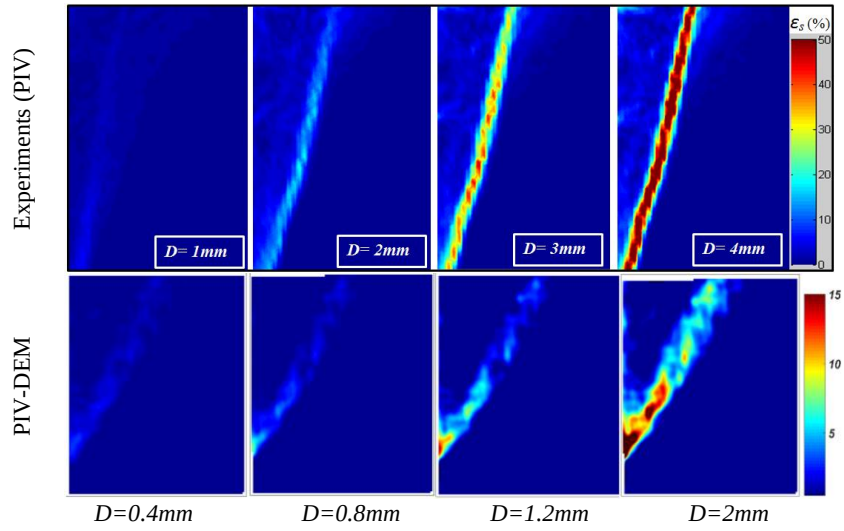

Figure 6. Shear strain distribution with respect to wall movement.

Using PIV, shear strain maps are obtained to further analyse the defamation location in the backfills. Figure 6 presents the consecutive stages of the test. It is observed that shear strain concentrates to a continuous region even during the initial stages of the test in both test cases (note based on observations in Figure 5, only results of paired particles are presented here). Furthermore, the slip surface becomes more distinct only with increasing wall movement. A close look also reveals that the inclination of the formed wedge is almost fixed and not changing by wall movement.

Additionally, considering the methodology discussed in Section 2.4, failure surfaces are quantified for both cases. Note that since measurements are normalized by the wall height, it is also possible to conduct a quantitative comparison. Figure 7 shows results of three backfills with distinct density states. It is obvious that dense sample leads to smaller wedges. This can be justified by the fact that denser packings yield higher internal friction angles, and thus, a smaller zone is subjected to failure. Considering DEM results, it can be seen that including shape factor (i.e. considering paired particles) leads change in geometry of the formed wedges. This observation highlights the importance of the interlocking effect among particles (which is obtained through considering the simplest non-spherical shape). Overall, it is seen that the failure surfaces in case of experimental results are much closer to the wall (this might be a direct indication of higher interlocking among natural sand particles). However, it must be noted that a detailed calibration process is needed to be able of performing a precise comparison.

4 CONCLUSIONS

Initially, the present study employed PIV method to enable visualisation of deformation localization in an experimental set-up. This way it became possible to detect the evolution of the failure surface formation within the cohesionless backfill. The backfills were prepared in different density states, which clarified the dependency of failure wedge on sample confinement. Results suggested that dense samples yield smaller wedges (due to presence of higher internal friction among particles).

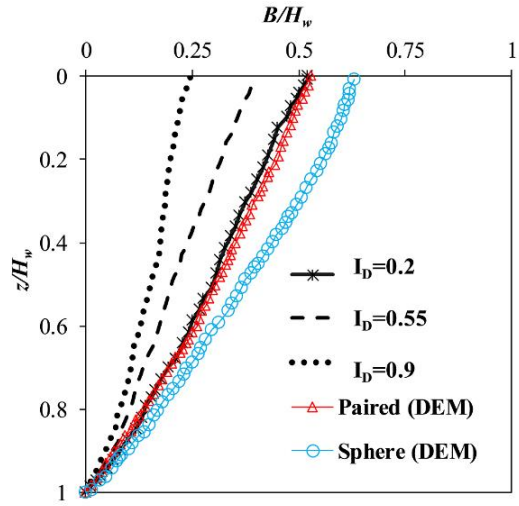

Figure 7. Comparison of the failure surface geometry.

Later, DEM is utilized to investigate the particle shape effect in a cohesionless backfill. The shape representation was addressed through two approaches (most simple shapes): spherical particles and clumped particles. It is already known that in the case of spheres, the mechanical interlocking is under-represented and the rotation of the individual particles is restricted merely by frictional forces. However, the clump particles couple both frictional forces and mechanical interlocking to hinder rotational freedom. This distinction enhanced the stability of the paired particles during failure, which resulted in a uniform velocity distribution for individual particles over a distinct area (thisi is inline with experimental observations). Consequently, it is pointed out that considering shape parameter is essential for predicting the realistic backfill properties.

In a future study we will consider the effect of increasing shape complexity and its effect on the macro-scale response of the backfill. Additionally, DEM parameters will be calibrated to enable further investigation regarding shear band characteristics and wall pressure distributions.

5 ACKNOWLEDGMENT

This research has been supported by Bogazici University Scientific Research Project BAP14501D.

6 REFERENCES

Adrian, R. J. 1991. Particle-imaging techniques for experimental fluid mechanics, *Annual Review of Fluid Mechanics* **23**, 261–304.

Coulomb, C. 1776. *Essai sur une application des regles des maximis et minimis a quelues problemes de statique relatifs a larchitecture*, De l'Imprimerie Royale.

Cundall, P. A., Strack, O. D. L. 1979. A discrete numerical model for granular assemblies, *Géotechnique* **29**, 47–65.

D. E. M. Solutions, 2014. *EDEM 2.6 Theory reference guide*, Edinburgh, UK.

Fang, Y., Ishibashi, I. 1986. Static earth pressures with various wall movements, *Journal of Geotechnical Engineering* **112**, 317–333.

Favier, J. F., Abbaspour-Fard, M. H., Kremmer, M., Raji, A. O. 1999. Shape representation of axi-symmetrical, non-spherical particles in discrete element simulation using multi-element model particles, *Engineering Computations* **16**, 467–480.

Lesniewska, D., Wood, D. M. 2009. Observations of Stresses and Strains in a Granular Material, *Journal of Engineering Mechanics* **135**, 1038–1054.

O'Sullivan, C. 2011. Particle-based discrete element modeling: geomechanics perspective, *International Journal of Geomechanics* **11**, 449–464.

Pietrzak, M., Leśniewska, D. 2012. Failure evolution in granular material retained by rigid wall in active mode, *Studia Geotechnica et Mechanica* **34**, 1–9.

Rankine, W. J. M. 1857. On the Stability of Loose Earth, *Proceedings of the Society of London* **147**, 9–27.

Soltanbeigi, B., Papanicolopulos, S. A., and Ooi, J. Y., 2016. Particle shape effect on deformation localization during quasi-static flow at active state." 5th Int. Conf. on Geot. Eng. and soil mech., Tehran, Iran.

Soltanbeigi, B., Podlozhnyuk, A., Papanicolopulos, S.A., Kloss, C., Pirker, S. and Ooi, J.Y., 2018. DEM study of mechanical characteristics of multi-spherical and superquadric particles at micro and macro scales. *Powder Technology* **329**, 288-303.

Spangler, M. G., Handy, R. L. 1982. *Soil engineering*, Harper and Row, New York.

Take, W. A., Bolton, M. D., White, D. J. 2003. Soil deformation measurement using particle image velocimetry (PIV) and photogrammetry, Géotechnique **53**, 619–631.

Terzaghi, K. 1943. *Theoretical soil mechanics*, Chap. 5, 66:76, Wiley.

Toyosawa, Y., Itoh, K., Tamrakar, S. B. 2006. Redistribution of active earth pressures using movable earth support apparatus in centrifuge, *Phys. Model. Geotech.–6th ICPMG*, no. 4, pp. 1113–1118.

Tsagareli, Z. V. 1965. Experimental investigation of the pressure of a loose medium on retaining walls with a vertical back face and horizontal backfill surface, *Soil Mechanics and Foundation Engineering* **2**, 197–200.

Wensrich, C. M., Katterfeld, A. 2012. Rolling friction as a technique for modelling particle shape in DEM, *Powder Technology* **217**, 409–417.